*Optica Applicata, Vol. XLVIII, No. 3, 2018*
10.5277/oa180312

# The fractal dimension of red blood cell aggregates in dextran 70 solutions

MACIEJ BOSEK[1], ALICJA SZOŁNA-CHODÓR[1], NADIA ANTONOVA[2], BRONISŁAW GRZEGORZEWSKI[1*]

[1]Department of Biophysics, Collegium Medicum in Bydgoszcz, Nicolaus Copernicus University, ul. Jagiellońska 15, 85-067 Bydgoszcz, Poland

[2]Department of Biomechanics, Institute of Mechanics, Bulgarian Academy of Sciences, Acad. G. Bonchev St., bl. 4, 1113 Sofia, Bulgaria

[*]Corresponding author: grzego@cm.umk.pl

Fractal dimension of three dimensional red blood cell aggregates were determined by measurement of their size and sedimentation velocity. The sedimentation of the aggregates was investigated with red blood cells suspended in dextran 70 solutions at concentrations from 2 to 5 g/dL, at hematocrit 5% and 10%. The aggregate velocity and size were measured using an image analysis technique. The velocity *vs.* radius dependence of the aggregates exhibited a scaling behavior. This behavior showed the fractal structure of the aggregates. It is shown that the fractal dimension of the three dimensional red blood cell aggregates depends on the dextran concentration in the suspension. This parameter exhibited a minimum at dextran concentration between 3 and 4 g/dL. Thus the fractal dimensions increased as the aggregation extent decreased. The obtained results show that the sedimentation experiment together with image analysis is a promising technique to determine the fractal dimension of the three dimensional red blood cell aggregates.

Keywords: red blood cells, aggregation, fractal dimension, dextran 70.

## 1. Introduction

The red blood cell (RBC) aggregation process has been very extensively investigated [1]. The RBC aggregates alter the blood flow which is very important from a physiological point of view [2]. For this reason both the mechanism of the aggregation as well as the properties of the formed aggregates have attracted the interest of many investigators. Many techniques to quantify RBC aggregation have been developed, however failure of some methods in quantifying aggregation has been reported [1]. Among the parameters of RBC aggregation, fractal dimension seems to be a good candidate to give additional knowledge about the process.

The adhesion of RBCs is the source of RBC aggregate formation. There are two models of the mechanism of adhesion between RBCs [3]. First of them, the bridging

model, involves plasma fibrinogen or polymers like dextran attaching to the glycocalyx of adjacent cells and building bridges between them. The second model, the depletion model, assumes that fibrinogen or polymers flow out from the gap between cells resulting in osmotic pressure joining these cells. Note that the measurements of the adhesion of RBCs give quantitative and precise information about interactions undergoing between the cells [4].

The RBC aggregation process has many steps, stages and manifestations. There are many factors participating in RBC aggregation and phenomena associated with this process [5–11]. In the first stage of the RBC aggregation process rouleaux are formed. There are techniques that provide information about the temporal changes of the size of the formed rouleaux. Especially there are methods to measure the number of erythrocytes in rouleaux at any given time of the process [6, 12, 13]. In the second stage of the RBC aggregation process rouleaux coalesce to form three dimensional red blood cell (3D RBC) aggregates. The size of the aggregates can be about 100 μm. The large aggregates exhibit a porous structure and the fractal dimension can be used as the quantitative measure of their structure.

In general, the fractal dimension of aggregates can be measured with the use of light or ultrasound scattering, settling and image analysis techniques [14, 15]. Johnson *et al*. showed that the method based on the Stokes equation gave appropriate fractal dimension of aggregates [15]. Bushel *et al*. have shown that the behavior of aggregate fractal dimension can be explained by numerical results [14]. They have shown that increasing binding energy increases the probability of binding of two objects after their contact. If that probability is high, the aggregation appears after first contacts giving tenuous aggregates with relatively low fractal dimension. Lower probability increases the mean number of contacts, yielding more compact aggregates with larger fractal dimension [14].

Up to now the fractal dimension of 3D RBC aggregates was determined in few studies by simple image analysis such as the modified box-counting method [16–18]. Meng-Zhen Kang *et al*. gave the first demonstration of fractal characteristic of 3D RBC aggregates [16]. Furthermore, they have shown that an increase of binding energy causes a decrease of Hausdorff dimension and argued that for this reason the Hausdorff dimension should be used to assess the binding energy. Rapa *et al*. using the box-counting method estimated the fractal dimension of 3D RBC aggregates [17]. Peng Kai Ong *et al*. studied horse blood and they have shown that the fractal dimension of RBC aggregates suspended in dextran 500 solutions decreased from 1.49 to 1.36 with increasing dextran concentration from 0 to 1.5 g/dL, where RBC aggregation increased [18]. In investigations of ultrasound scattering in RBC suspensions, the fractal dimension of RBC aggregates was considered [19–21]. Recently, preliminary results of the fractal dimension of 3D RBC aggregates incubated previously in glucose solutions were obtained using techniques based on the measurement of the sedimentation velocity [22].

In this study, we investigated the fractal structure of sedimenting 3D RBC aggregates in dextran solutions, based on their sedimentation velocity *vs.* the mean radius behavior. In our earlier studies, the various techniques of 3D RBC aggregates velocity

measurements were proposed [22–24]. In this study, the velocity was measured using Fourier's method and the size of the aggregates were obtained from intensity correlation in the image of the aggregates. The scaling behavior of the dependence of sedimentation velocity from mean radius of aggregates is analyzed. Our purpose was to interpret this behavior using fractal geometry. The effect of dextran concentrations on aggregate fractal dimension is investigated. Finally, the correlation between obtained fractal dimension and erythrocyte agreeability is discussed.

## 2. Materials and methods

Venous blood was drawn from adult healthy volunteers from the local blood center in sterile tubes containing $K_3$EDTA anticoagulant and stored at 4°C. The whole blood was centrifuged at 3000 rpm for 5 min at 4°C, next the plasma and buffy coat was discarded. To eliminate proteins, the RBCs were washed three times with phosphate buffer saline (PBS: pH 7.4) at the previous settings of a centrifuge. RBCs were used to obtain samples of suspensions in dextran 70 kDa solution at concentrations 2, 3, 4 and 5 g/dL in PBS at hematocrit 5% and 10%. At given hematocrit and dextran concentration, six samples for different donors were prepared. Samples were gently mixed and injected into the container. The experimental setup used in this study is shown in Fig. 1. The white LED lamp illuminating the ground glass was a light source providing uniform brightness of the sample. The sample was placed into a rectangular glass-walled container of 18 × 23 × 1 $mm^3$ (width × height × depth). The image of the sample was focused by an objective and registered every second by the CCD camera (2592 × 1944 pixels), where the fragments of the image sized 2.9 × 2.9 $mm^2$ (1000 × 1000 pixels) covering the center of the container were investigated. Each measurement lasted for 3000 seconds or less if the observed processes finished much earlier. Experiments were made at room temperature (22°C). The experiments were carried out according to the ethical guidelines laid down by the local bioethical commission.

The Fourier technique used to determine the velocity of the 3D RBC aggregates is schematically shown in Figs. 2 and 3. The images of the suspensions were taken every 1 s. Examples of the images are shown in the top of Fig. 2. From each of the images, the single column of the pixels at the same position was selected. Next a pattern of temporal sequence of pixel columns was constructed. The temporal sequence consists of the columns ordered in time. The temporal sequence of the columns is shown

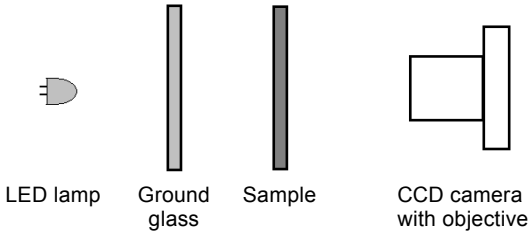


Fig. 1. Experimental setup.

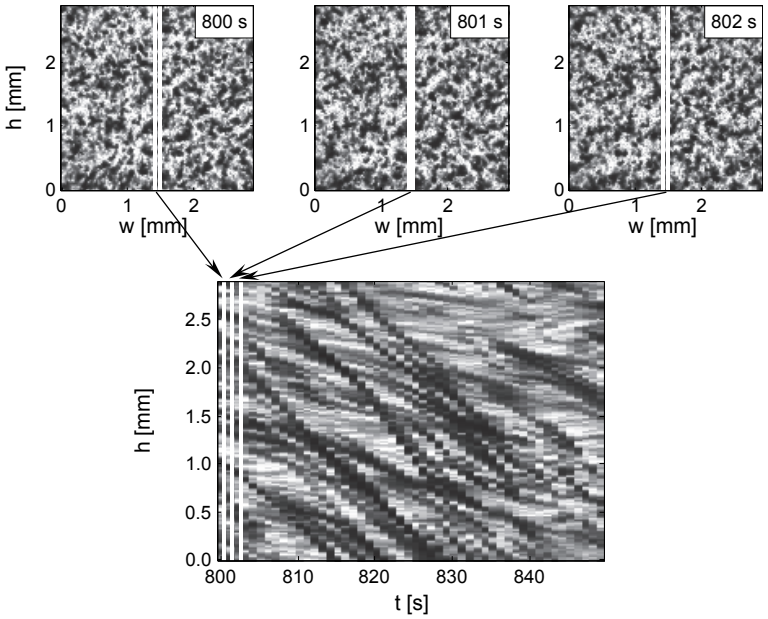


Fig. 2. Composition of sequence of pixel columns from fragments of successive sample images of RBC suspension at hematocrit 10% and dextran concentration 3 g/dL.

in the bottom of Fig. 2. This sequence shows the aggregate vertical positions as functions of time. The slopes of these functions are equal to the velocities of the aggregates. The mean velocity of aggregates can be measured using the Fourier transform of these sequences [23]. The transform of the temporal sequences of 50 pixel columns is shown in Fig 3**a**. To average the velocity of the aggregates, the procedure was repeated for pixel columns at each position in the images. Then the square moduli of obtained trans-

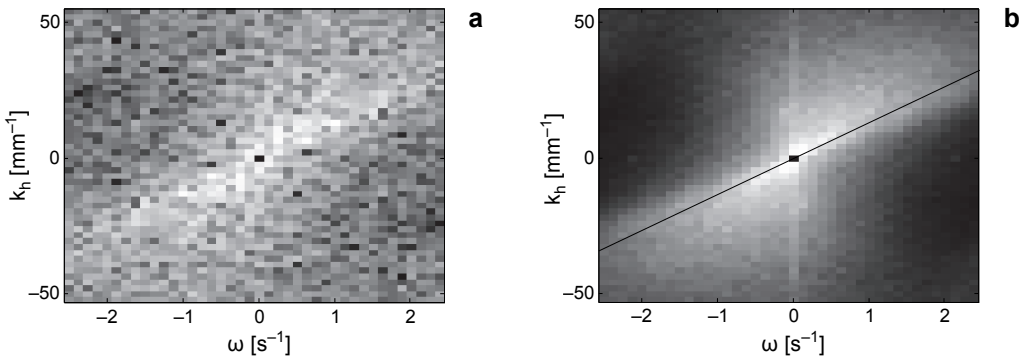


Fig. 3. Fourier transforms of sequences of pixel columns for one column position (**a**) and square modulus of these transforms averaged over each column positions (**b**) for RBC suspension at hematocrit 10% and dextran concentration 3 g/dL. The line passes through the transform at the direction in which it was widest. The slope of the line determines the average velocity of RBC aggregates.

forms were averaged. The averaged transform was shown in Fig. 3**b**. In the Fourier transform one can observe that high values appeared from the down left part to the upper right part of the plot. These high values of the Fourier transform correspond to the orientation of functions observed in the plot of the column sequences. Since these functions are almost parallel, the line passing through those high values can be introduced. The slope of this line is inversely proportional to the mean slop of functions in the plot of the column sequence [25]. Thus the slope of the introduced line determines the average velocity of the aggregates.

The aggregate size was measured using vertical correlation function of the intensity in the sample images. The example of the correlation function was shown in Fig. 4. The correlation functions were averaged for images in a given temporal sequence. Finally, the exponential function $C(\Delta h) \sim \exp(-\Delta h/r_a)$ was fitted to the obtained average correlation function, where $\Delta h$ is the vertical displacement and $r_a$ is the correlation length, which is a mean aggregate radius estimation.

The theoretical description of the settling velocity of an isolated RBC aggregate is given by terminal velocity in the presence of gravity, buoyancy and Stokes forces, since due to the high Peclet number and low Reynolds number of sedimenting aggregates, their motion is practically unaffected by inertial and thermal effects. From the equilibrium of these forces for fully packed aggregates, the settling velocity can be given by $u_a \sim r_a^2$, where $r_a$ is the aggregate radius. However, since the aggregates consist of erythrocytes and solution between them, and the contribution of erythrocytes in aggregate volume decreases with $r_a$, *i.e.* the number of erythrocytes in aggregate $N_e$ does not increase with the third power of aggregate radius, the aggregates exhibit the fractal structure. Then the following scaling relationship can be introduced [15]: $N_e \sim r_a^D$, where $D$ is an aggregate fractal dimension. This dependence yields the relation for aggregate velocity [15]: $u_a \sim r_a^{D-1}$. This velocity was derived for particles settling without any interaction with other particles. In the system of collective sedimentation of many particles, the velocity was additionally affected by a hindrance effect due to

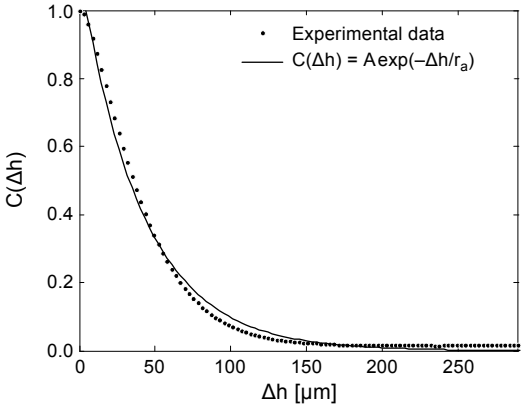


Fig. 4. The spatial correlation of the intensity in the sample images of RBC suspension at hematocrit 10% and dextran concentration 3 g/dL used to assess the aggregate size.

fluid backflow. The experimental [26] and theoretical [27] relations between the velocity of isolated and non-isolated particle were well known. These relations in general have the following form: $v = uf(\varphi)$, where $v$ and $u$ are the velocities for, respectively, non-isolated and isolated particle and $f(\varphi)$ is a function of volume fraction $\varphi$, given in our case by hematocrit. Assuming that the volume fraction is constant in the investigated phase of the process, the mean velocity of non-isolated aggregates of mean radius $r_a$ is given by: $v_a \sim r_a^{D-1}$.

## 3. Results

The sequences of columns from images of a whole sample obtained at hematocrit 5% and 10% and dextran concentration 3 g/dL were shown in Fig. 5. On both images initially no motion was observed because rouleaux were formed in the suspension. The resolving power of the optical system is limited so that small linear or branched aggregates cannot be observed. Next at time ~500 and ~300 s at hematocrit 5% and 10%, respectively, the formation of 3D RBC aggregates takes place and these large aggregates become visible. Immediately after their appearing they began to sediment. The time of the beginning of 3D RBC aggregates formation was similar at each height of the sample, whereas, the time of finishing of that phase decreased with increasing height. Especially, this can be seen in Fig. 5**b**. At a middle height of investigated sample, the sedimentation of large aggregates finished at ~1300 and ~800 s at hematocrit 5% and 10%, respectively. After finish of that phase only sparse small aggregates can be observed.

At the bottom of the sample the deposit of packed cells was observed as the dark area of low intensity, whereas, at the top, the region of sedimenting 3D RBC aggregates can be seen. In contrast to sedimentation at physiological hematocrit, no clear solution exists in the upper part of the container. The falling aggregates cause growth of the deposit. When the sedimentation of the large RBC aggregates finished, the height of

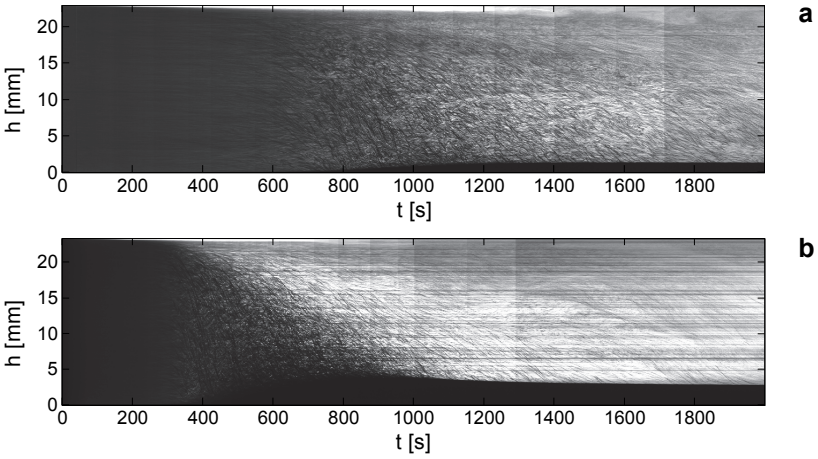


Fig. 5. The sequences of columns covering the whole measurement time from images of a whole sample of RBC suspensions at dextran concentration 3 g/dL and hematocrit 5% (**a**) and 10% (**b**).

the deposit reached a maximum. Later, decreasing of the height of the deposit manifests the final packing of the structure.

The RBC aggregate radius and velocity as functions of time at hematocrit 5% and 10% and dextran concentration 3 g/dL were shown in Fig. 6. It can be seen that after the start of sedimentation both parameters increased. Next they attained a maximum

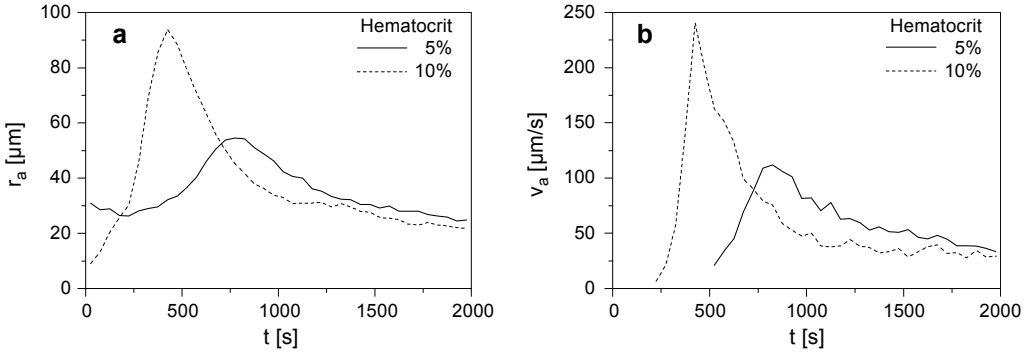


Fig. 6. The RBC aggregate radius (**a**) and velocity (**b**) as functions of time at hematocrit 5% and 10% and dextran concentration 3 g/dL.

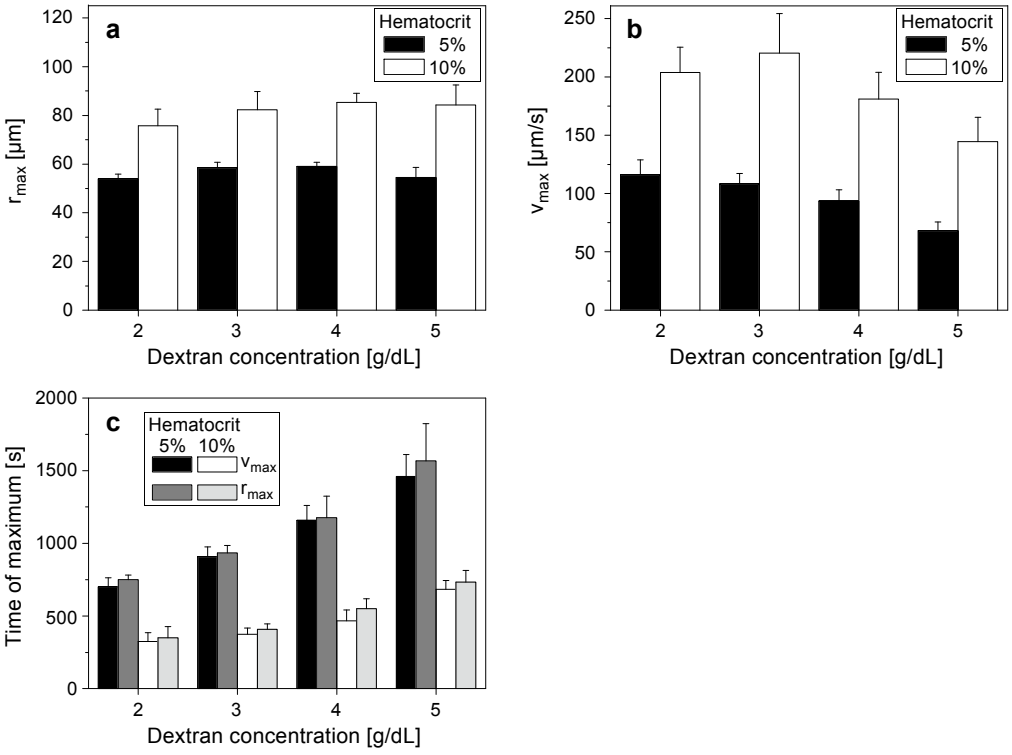


Fig. 7. The mean and standard deviation of maximal values of aggregate radius (**a**), velocity (**b**) and the times of achieving of these values (**c**) for investigated dextran concentration at hematocrit 5% and 10%.

and began to decrease. The increase of radius and consequently velocity in the first aggregation phase showed the predominance of the aggregate formation over their sedimentation. The decrease of the radius in the second sedimentation phase indicates that aggregate sedimentation overcame the aggregate formation. The aggregation causes increase of mean aggregate radius whereas the sedimentation occurring faster for larger aggregates, decreases mean aggregate size. The maximal values of aggregate radius, velocity and the times at which these values were attained, were shown in Fig. 7 for investigated dextran concentrations. At both values of hematocrit, the times of appearance of both, maximal aggregate radius and velocity increased with increasing dextran concentrations. At hematocrit 5% these values were similar, whereas at 10% the times for radius were smaller than that for velocity. For both values of hematocrit the maximal values of aggregate radius exhibited maximum at 4 g/dL. The maximal values of the aggregate velocity at hematocrit 5% decreased with dextran concentrations, whereas, at hematocrit 10%, these values exhibited a maximum at concentration 3 g/dL.

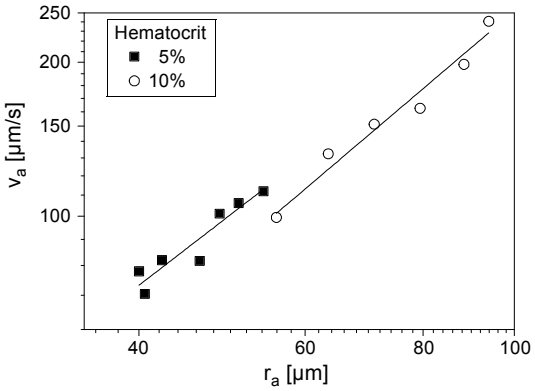


Fig. 8. The sedimentation velocity of aggregates *vs.* their mean radius in phase of sedimentation of large aggregates at hematocrit 5% and 10% and dextran concentration 3 g/dL.

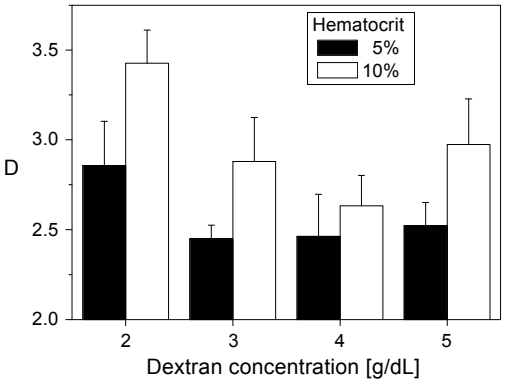


Fig. 9. The means and standard deviations of fractal dimension for investigated dextran concentration at hematocrit 5% and 10%.

The dependence of sedimentation velocity of aggregates on their mean radius in the phase of sedimentation of large aggregates was shown in Fig. 8 in the log–log plot, for the same samples as for velocity and radius time dependence in Fig. 7. The sedimentation velocity $v_a$ *vs.* radius $r_a$ of 3D RBC aggregates exhibited scaling behavior $v_a \sim r_a^{D-1}$. The fractal dimension $D$ for investigated samples was estimated from fitting of the power functions to experimental plots and are shown in Fig. 9. This parameter for hematocrit 10% exhibited a clear inverted bell-shape dependence on dextran concentration. The fractal dimension initially decreased and next increased with increasing dextran concentration, attaining a minimal value at concentration ~4 g/dL. For hematocrit 5% at smaller dextran concentrations similar behavior was observed. This parameter after initial decreasing, attained a minimum at concentration ~3 g/dL.

## 4. Discussion

In this study we confirm the fractal structure of 3D RBC aggregates. A sedimentation technique to determine the fractal dimension of the aggregates is proposed. The fractal dimension is a parameter giving information about the RBC aggregability. This parameter was obtained from sedimentation velocity *vs.* mean radius behavior for aggregates of RBCs suspended in dextran solutions.

During RBC sedimentation various phenomena and structures formed by the cells occur. At the first stage of the sedimentation process, rouleaux formation takes place. In the next stage 3D RBC aggregates form and sediment. During the 3D RBC aggregate formation the growth of their size and an increase in their falling velocity is observed. When the formation of the aggregates is completed, the parameters take maximum values. Next the sedimentation of the formed aggregates takes place and this stage is investigated in detail in this paper. The scaling behavior of the sedimentation velocity of the formed aggregates *vs.* their mean radius confirms the fractal nature of the aggregates. From the relationship, the fractal dimension of the aggregates was determined.

To show the correspondence between the extent of aggregation and fractal dimension of the aggregates, the sedimentation of RBCs in dextran solutions was investigated. The study of the dependence of RBC aggregation in dextran solution on its concentration has a long history [4, 28–32]. The characteristic bell-shape of the data for the relationship was found with the use of different methods and techniques. Especially for dextran 70, the RBC aggregation attains a maximum at concentration between 3 and 4 g/dL. From this study, a reverse behavior for the fractal dimension was seen. Higher fractal dimension of the 3D RBC aggregates was observed at lower and higher dextran concentrations while the minimum value for the fractal dimension was obtained at the concentration responsible for the maximum of the RBC aggregation. The behavior of fractal dimensions of 3D RBC aggregates investigated in this study with the use of sedimentation techniques can be compared with the behavior of the dimension determined using imaging techniques [18]. Peng Kai Ong *et al*. have shown the negative correlation between the aggregation index and the fractal dimension of the aggregates of horse RBCs formed in dextran 500 solution [18]. Furthermore they have shown this

negative correlation in the case when dextran 40 was added to the solution to decrease the aggregation. It shows a correspondence between the results obtained by the imaging technique and ones obtained with the sedimentation technique used in this study.

Obtained fractal dimension can be also interpreted according to the results of numerical simulation presented by Bushell *et al*. [14] and Meng-Zhen Kang *et al*. [16]. They have found that increasing binding energy between RBCs causes a decrease of the fractal dimension of resultant aggregates. Thus obtained in our study changes of fractal dimension can be interpreted as a result of changes of binding energy. Our results indicate that maximum of binding energy appears at dextran concentration between 3 and 4 g/dL. The binding energy between RBCs suspended in dextran solutions was earlier estimated by other authors assuming bridging as well as depletion models [29, 31]. They have obtained experimentally and theoretically the dependence of the binding energy from dextran concentration. The dependence for dextran 70 achieved by these authors corresponds with our data.

Finally let us consider the effect of hematocrit of the RBC suspension on the fractal dimension of appeared aggregates. The fractal dimension of the aggregates at hematocrit 10% is little higher than the dimension obtained at hematocrit 5% but the dependence of the dimension on the dextran concentration is similar in both cases. Furthermore, for dextran concentration 2 g/dL at hematocrit 10%, the fractal dimension exceeded its possible maximum value. It suggests the existence of the mechanism, more apparent at higher hematocrit, that at the beginning of the sedimentation phase causes an increase of the velocity of the largest aggregates above the value predicted by the above theoretical considerations.

## 5. Conclusion

In this study, for the first time the fractal dimension of sedimenting 3D RBC aggregates was estimated. The fractal dimension of the aggregates exhibits an inverted bell-shape dependence from dextran 70 concentration, taking a minimum value between 3 and 4 g/dL. It additionally shows that the fractal dimensions of the 3D RBC aggregates can be a measure of the binding energy between erythrocytes. This suggests that the fractal dimension of the 3D RBC aggregates and presented sedimentation techniques for its determination can give an important insight into the field of RBC aggregation.

### References

[1] Baskurt O., Neu B., Meiselman H.J., *Red Blood Cell Aggregation*, CRC Press, Boca Raton, 2011.

[2] Yalcin O., Uyuklu M., Armstrong J.K., Meiselman H.J., Baskurt O.K., *Graded alterations of RBC aggregation influence in vivo blood flow resistance*, American Journal of Physiology – Heart and Circulatory Physiology 287(6), 2004, pp. H2644–H2650.

[3] Bäumler H., Neu B., Donath E., Kiesewetter H., *Basic phenomena of red blood cell rouleaux formation*, Biorheology **36**(5–6), 1999, pp. 439–442.

[4] Steffen P., Verdier C., Wagner C., *Quantification of depletion-induced adhesion of red blood cells*, Physical Review Letters 110(1), 2013, article ID 018102.

[5] Game L., Voegel J.C., Schaaf P., Stoltz J.F., *Do physiological concentrations of IgG induce a direct aggregation of red blood cells: comparison with fibrinogen*, Biochimica et Biophysica Acta (BBA) – General Subjects 1291(2), 1996, pp. 138–142.
[6] Kernick D., Jay A.W.L., Rowlands S., Skibo L., *Experiments on rouleau formation*, Canadian Journal of Physiology and Pharmacology 51(9), 1973, pp. 690–699.
[7] Fenech M., Garcia D., Meiselman H.J., Cloutier G., *A particle dynamic model of red blood cell aggregation kinetics*, Annals of Biomedical Engineering 37(11), 2009, pp. 2299–2309.
[8] Sehyun Shin, Yun-Hee Ku, Jang-Soo Suh, Singh M., *Rheological characteristics of erythrocytes incubated in glucose media*, Clinical Hemorheology and Microcirculation **38**(3), 2008, pp. 153–161.
[9] Zilberman-Kravits D., Harman-Boehm I., Suster T., Meyerstein N., *Increased red cell aggregation is correlated with $HbA_{1C}$ and lipid levels in type 1 but not type 2 diabetes*, Clinical Hemorheology and Microcirculation **35**(4), 2006, pp. 463–471.
[10] Antonova N., Riha P., Ivanov I., *Time dependent variation of human blood conductivity as a method for an estimation of RBC aggregation*, Clinical Hemorheology and Microcirculation 39(1–4), 2008, pp. 69–78.
[11] Kaliviotis E., *Mechanics of the red blood cell network*, Journal of Cellular Biotechnology 1(1), 2015, pp. 37–43.
[12] Barshtein G., Wajnblum D., Yedgar S., *Kinetics of linear rouleaux formation studied by visual monitoring of red cell dynamic organization*, Biophysical Journal 78(5), 2000, pp. 2470–2474.
[13] Szołna-Chodór A.A., Bosek M., Grzegorzewski B., *Kinetics of red blood cell rouleaux formation studied by light scattering*, Journal of Biomedical Optics 20(2), 2015, article ID 025001.
[14] Bushell G.C., Yan Y.D., Woodfield D., Raper J., Amal R., *On techniques for the measurement of the mass fractal dimension of aggregates*, Advances in Colloid and Interface Science 95(1), 2002, pp. 1–50.
[15] Johnson C.P., Xiaoyan Li, Logan B.E., *Settling velocities of fractal aggregates*, Environmental Science and Technology 30(6), 1996, pp. 1911–1918.
[16] Meng-Zhen Kang, Yan-Jun Zeng, Jian-Gang Liu, *Fractal research on red blood cell aggregation*, Clinical Hemorheology and Microcirculation **22**(3), 2000, pp. 229–236.
[17] Rapa A., Oancea S., Creanga D., *Fractal dimensions in red blood cells*, Turkish Journal of Veterinary and Animal Sciences **29**(6), 2005, pp. 1247–1253.
[18] Peng Kai Ong, Swati Jain, Bumseok Namgung, Sangho Kim, Keyoung Jin Chun, Jun-Uk Chu, Dohyung Lim, *Study of time-dependent characteristics of a syllectogram in the presence of aggregation inhibition*, International Journal of Precision Engineering and Manufacturing 13(3), 2012, pp. 421–428.
[19] Lim B., Cobbold R.S.C., *On the relation between aggregation, packing and the backscattered ultrasound signal for whole blood*, Ultrasound in Medicine and Biology 25(9), 1999, pp. 1395–1405.
[20] Haider L., Snabre P., Boynard M., *Rheology and ultrasound scattering from aggregated red cell suspensions in shear flow*, Biophysical Journal 87(4), 2004, pp. 2322–2334.
[21] Snabre P., Haider L., Boynard M., *Ultrasound and light scattering from a suspension of reversible fractal clusters in shear flow*, The European Physical Journal E 1(1), 2000, pp. 41–53.
[22] Szołna-Chodór A., Bosek M., Grzegorzewski B., *Effect of glucose on formation of three dimensional aggregates of red blood cells*, Series on Biomechanics **29**(4), 2015, pp. 20–26.
[23] Grzegorzewski B., Kempczyński A., *Blood aggregate size and velocity during blood sedimentation*, Proceedings of SPIE 6254, 2006, article ID 62541H.
[24] Kempczyński A., Grzegorzewski B., *Estimation of red blood cell aggregate velocity during sedimentation using the Hough transform*, Optics Communications 281(21), 2008, pp. 5487–5491.
[25] Goodman J.W., *Introduction to Fourier Optics*, McGraw-Hill Book Company, San Francisco, 1968.
[26] Richardson J.F., Zaki W.N., *Sedimentation and fluidization: Part I*, Transactions of the Institution of Chemical Engineers **32**, 1954, pp. 35–53.
[27] Batchelor G.K., *Sedimentation in a dilute dispersion of spheres*, Journal of Fluid Mechanics 52(2), 1972, pp. 245–268.

[28] Antonova N., Riha P., Ivanov I., *Experimental evaluation of mechanicaland electrical properties of RBC suspensions under flow. Role of RBC aggregating agent*, Clinical Hemorheology and Microcirculation 45(2–4), 2010, pp. 253–261.
[29] Neu B., Meiselman H.J., *Depletion-mediated red blood cell aggregation in polymer solutions*, Biophysical Journal 83(5), 2002, pp. 2482–2490.
[30] Meiselman H.J., Neu B., Rampling M.W., Baskurt O.K., *RBC aggregation: laboratory data and models*, Indian Journal of Experimental Biology **45**(1), 2007, pp. 9–17.
[31] Buxbaum K., Evans E., Brooks D.E., *Quantitation of surface affinities of red blood cells in dextran solutions and plasma*, Biochemistry 21(13), 1982, pp. 3235–3239.
[32] Barshtein G., Tamir I., Yedgar S., *Red blood cell rouleaux formation in dextran solution: dependence on polymer conformation*, European Biophysics Journal 27(2), 1998, pp. 177–181.

*Received December 20, 2017*